

HIGH-ENERGY GAMMA-RAY ACTIVITY FROM V404 CYGNI DETECTED BY AGILE DURING THE 2015 JUNE OUTBURST

G. PIANO,¹ P. MUNAR-ADROVER,¹ F. VERRECCHIA,^{2,3} M. TAVANI,^{1,4,5} AND S. A. TRUSHKIN^{6,7}

¹*INAF-IAPS, Via del Fosso del Cavaliere 100, I-00133, Roma, Italy*

²*ASI Data Center (ASDC), Via del Politecnico snc, I-00133, Roma, Italy*

³*INAF-OAR, Via di Frascati 33, I-00040 Monte Porzio Catone (RM), Italy*

⁴*INFN Roma Tor Vergata, Via della Ricerca Scientifica 1, I-00133, Roma, Italy*

⁵*Dipartimento di Fisica, Università di Roma “Tor Vergata”, Via Orazio Raimondo 18, I-00173 Roma, Italy*

⁶*Special Astrophysical Observatory RAS, Karachaevo-Cherkassian Republic, Nizhnij Arkhyz 36916, Russian Federation*

⁷*Kazan Federal University, Kazan 420008, Russian Federation*

ABSTRACT

The AGILE satellite detected transient γ -ray activity from the X-ray binary V404 Cygni, during the June 2015 outburst observed in radio, optical, X-ray and γ -ray frequencies. The high-energy γ -ray emission was observed by AGILE in the 50–400 MeV energy band, between 2015-06-24 UT 06:00:00 and 2015-06-26 UT 06:00:00 (MJD 57197.25–57199.25), with a detection significance of $\sim 4.3\sigma$. The γ -ray detection, consistent with a contemporaneous observation by *Fermi*-LAT, is correlated with a bright flare observed at radio and hard X-ray frequencies, and with a strong enhancement of the 511 keV line emission, possibly indicating plasmoid ejections in a lepton-dominated transient jet. The AGILE observations of this binary system are compatible with a microquasar scenario in which transient jets are responsible for the high-energy γ -ray emission.

Keywords: gamma-rays: stars, X-rays: binaries, stars: black holes, stars: jets

1. INTRODUCTION

V404 Cygni (hereafter V404 Cyg), also known as GS 2023+338, is a low mass X-ray binary (LMXB) located at a distance of 2.39 ± 0.14 kpc, accurately inferred by a parallax measurement (Miller-Jones et al. 2009). The system is composed of a $9^{+0.2}_{-0.6} M_{\odot}$ black hole (BH) and a $0.7^{+0.3}_{-0.2} M_{\odot}$ K3 III companion star with an orbital period of 6.4714 ± 0.0001 days (Casares et al. 1992) and a 67° inclination with respect to the line of sight (Casares & Charles 1994; Shahbaz et al. 1994; Khargharia et al. 2010). V404 Cyg was discovered as a nova during an optical outburst in 1938, and it was observed for the first time in the X-ray band by the GINGA satellite, during an intense outburst in 1989 (Makino et al. 1989).

LMXBs are usually transient systems, showing long periods of quiescence (years), with faint and rapidly variable emission in the X-ray and radio frequencies (Miller-Jones et al. 2008; Hynes et al. 2009; Rana et al. 2016), and bright outburst states (weeks/months). The X-ray luminosities span from 10^{31-33} erg s $^{-1}$ during quiescence phase up to Eddington limit ($L_{\text{Edd}} \approx 10^{39}$ erg s $^{-1}$ for a $9 M_{\odot}$ BH) in the outburst states (Rodríguez et al. 2015).

After a quiescence period of ~ 26 years, the detection by *Swift*/BAT triggered the observations of a new active phase on 2015 June 15 (MJD 57188, Barthelmy et al. 2015) that lasted ~ 2 weeks and was observed across all wavelengths (from radio to soft γ -rays), with a highly variable emission (Trushkin et al. 2015; Rodríguez et al. 2015; Jenke et al. 2016). The correlated variability between optical and X-ray emissions during the bright June 2015 activity has been interpreted as a consequence of the instability of its large accretion disk (the outer accretion disk radius is $R_{\text{out}} \sim 10^7$ km). A disruption of the accreting mass inflow into the inner part of the disk can represent a critical factor to explain the observed scenario of this intense outburst: large-amplitude fluctuations which rapidly ended after only two weeks. The outburst possibly started in the innermost part of the disk, but it was not sustained by the accretion. The mass inflow could be disrupted either by a low surface density in the outer part of the disk – because of its long orbital period (Kimura et al. 2016) – or by a strong outer-disk wind regulating the accretion (Muñoz-Darias et al. 2016).

In June 2015, besides optical and X-ray intense variable emissions, indicating the combined activity of the corona-disk system, observations in radio (Trushkin et al. 2015) and γ -ray energies (Siegert et al. 2016; Loh et al. 2016) confirmed the ejection of relativistic plasma jets. In particular, hints of $e^+ e^-$ pair

annihilation, which are consistent with a microquasar scenario, have been found by INTEGRAL during the active phase (Siegert et al. 2016).

In this paper we present the AGILE observations of V404 Cyg during the peak phase of this intense activity, compare the results with the *Fermi*-LAT data, and analyze the high-energy (HE) γ -ray emission in a multi-wavelength context.

2. OBSERVATIONS AND DATA ANALYSIS

We analyzed the data collected by the *GRID* (Gamma-Ray Imaging Detector, Barbiellini et al. 2002; Prest et al. 2003), the γ -ray silicon-tracker imager on board the AGILE satellite (for a detailed description of the AGILE payload: Tavani et al. 2009a), and we compared our results with the *Fermi*-LAT observations of the system (see Appendix A).

The AGILE-*GRID* is sensitive to γ -ray photons in the energy range 30 MeV – 30 GeV. The point spread function (PSF) at 100 MeV and 400 MeV is 4.2° and 1.2° (68% containment radius), respectively (Sabatini et al. 2015). AGILE had operated in a “pointing” mode data-taking, characterized by fixed attitude observations, until November 2009, when the satellite entered in “spinning” mode, covering a large fraction of the sky with a controlled rotation of the pointing axis. In this current observing mode, typical 2-day integration-time sensitivity (3σ) for sources in the Galactic plane and photon energy above 100 MeV is $\sim 10^{-6}$ photons cm $^{-2}$ s $^{-1}$.

The analysis of the AGILE-*GRID* data was carried out with the new `Build_23` scientific software, FM3.119 calibrated filter and I0025 response matrices. The consolidated archive, available from the ASI Data Center (ASDCSTDk), was analyzed by applying South Atlantic Anomaly event cuts and 80° Earth albedo filtering. Only incoming γ -ray events with an off-axis angle lower than 60° were selected for the analysis. Statistical significance and flux determination of the point sources were calculated by using the AGILE multi-source likelihood analysis (MSLA) software (Bulgarelli et al. 2012) based on the Test Statistic (TS) method as formulated by Mattox et al. 1996. This statistical approach provides a detection significance assessment of a γ -ray source by comparing maximum-likelihood values of the null hypothesis (no source in the model) with the alternative hypothesis (point source in the field model). In this work we report 68% confidence level (C. L.) flux upper limits (ULs) if $\text{TS} < 9$ (detection significance $\lesssim 3$) and flux values with the corresponding 1σ statistical errors otherwise ($\text{TS} \geq 9$).

Before analyzing the outburst interval, we carried out an analysis of the Cygnus field during a 5-month pe-

riod between 2015-01-01 UT 12:00:00 and 2015-06-01 UT 12:00:00. The analysis took into account two different energy bands: 50–400 MeV and above 400 MeV. This preliminary analysis allowed us to model the γ -ray field just before the onset of the strong activity from V404 Cyg. For both energy ranges we performed a MSLA including – in addition to V404 Cyg – the 3 main pulsars of the Cygnus region (PSR J2021+3651, PSR J2021+4026 and PSR J2032+4127), which are known to be intense and persistent γ -ray sources. We modeled the γ -ray spectrum for V404 Cyg by assuming a simple power law with a 2.1 photon index¹. Flux ULs of 1×10^{-7} photons $\text{cm}^{-2} \text{s}^{-1}$ and 2×10^{-8} photons $\text{cm}^{-2} \text{s}^{-1}$ were found for V404 Cyg in 50–400 MeV and >400 MeV energy bands, respectively. The fluxes of the 3 γ -ray pulsars, found in these 5-month preliminary analyses, were kept fixed in the following MSLAs for the outburst phase. Furthermore, the diffuse emission (Galactic and extragalactic) quantified in this preliminary analysis was kept fixed during the study of the active period (June 2015).

For the outburst activity period we analyzed the time interval from 2015-06-20 UT 06:00:00 to 2015-06-30 UT 06:00:00, across the giant flare recorded by *Swift*/BAT (Segreto et al. 2015) and RATAN-600 (Trushkin et al. 2015) on 2015 June 26 (MJD 57199). A 48-hours bin light-curve for V404 Cyg was calculated (with a MSLA approach) in both energy bands. We selected these period (five 48-hours time intervals) in order to ensure a stable exposure for the target source. In the 50–400 MeV energy band, the on-source exposure for each bin was found to be almost constant around a value of $\sim 5.16 \times 10^6 \text{ cm}^2 \text{s}$ with a mean fluctuation of $\sim 3\%$. No detection with $\text{TS} > 9$ was found in the >400 MeV energy band, with 48h flux ULs lower than 5×10^{-7} photons $\text{cm}^{-2} \text{s}^{-1}$.

In the 50–400 MeV energy band a detection was found in the time interval between 2015-06-24 UT 06:00:00 and 2015-06-26 UT 06:00:00 (MJD 57197.25–57199.25), at Galactic coordinates $(l, b) = (72.41^\circ, -2.75^\circ) \pm 0.97^\circ$ (stat.) $\pm 0.10^\circ$ (syst.), with $\text{TS} = 18.1$ ($\sim 4.3\sigma$) and a γ -ray flux $F_\gamma = (4.6 \pm 1.5) \times 10^{-6}$ photons $\text{cm}^{-2} \text{s}^{-1}$ (see Fig. 1 and 6)². In the *left panel* of Fig. 2 the corresponding AGILE-GRID γ -ray intensity map is shown, with the result of the best-fitting position. The nominal position of V404 Cyg is within the error ellipse of the

AGILE γ -ray excess. The time correlation with the peak outburst phase observed in other wavelengths gives robustness to the association with V404 Cyg (see Section 3.1). For comparison, the *right panel* shows the quiescent phase of V404 Cyg as detected between 2015-01-01 UT 12:00:00 and 2015-06-01 UT 12:00:00.

In Fig. 3 the AGILE differential γ -ray spectrum (50 MeV – 1 GeV) for V404 Cyg during the 48h peak **activity is shown. No significant γ -ray emission is detected above 400 MeV.**

The γ -ray peak emission detected by AGILE is compatible in time with our analysis of *Fermi*-LAT data ($\text{TS} = 13.4$, MJD 57198.75–59199.75) in the 60–400 MeV energy band. Furthermore, our findings are consistent with the *Fermi*-LAT observations published in Loh et al. 2016. For a detailed description of our independent *Fermi*-LAT data analysis see Appendix A. A comparison between the AGILE-GRID and *Fermi*-LAT observations and findings is presented in Appendix A.1.

3. DISCUSSION

3.1. AGILE results in a multi-wavelength context

In Fig. 1 we plotted the AGILE-GRID light-curve together with published data from RATAN-600 (Trushkin et al. 2015), INTEGRAL/SPI (Siebert et al. 2016), and *Swift*/BAT³. A plot showing the time evolution of the radio spectral index α (where $S \sim \nu^\alpha$ is the radio flux density), in the band 4–11 GHz, is shown, reporting a change between an optically thick ($\alpha > 0$) and an optically thin ($\alpha < 0$) regime. Such variations could indicate a multiple plasmoid ejection in the jet. In Fig. 5 the radio spectrum, as detected by RATAN-600 during the outburst phase (MJD 57198.93), shows a change between an optically thick and an optically thin regime at ~ 4 GHz.

There is a simultaneity of the peak emission detected by AGILE (and *Fermi*-LAT), INTEGRAL/SPI (continuum 100–200 keV and annihilation emission), *Swift*/BAT (15–50 keV) and RATAN-600 (2.4–21.7 GHz). The γ -ray flare, detected by the AGILE-GRID between 50 and 400 MeV, occurs at MJD 57198.25 \pm 1, with an integration time including the preparation and prompt phase of the prominent burst detected in radio and hard X-ray frequencies (2015 June 26, MJD 57199). The multiwavelength pattern is very similar to the Cyg X-3 evolution around the γ -ray flare (Tavani et al. 2009b; *Fermi* LAT Collaboration et al. 2009; Corbel et al. 2012; Piano et al. 2012), and it is

¹ This is a standard value used in the AGILE analysis for unknown-spectrum or low-statistics sources (see Pittori et al. 2009).

² The systematic errors on flux measurements for AGILE have been quantified in 10% of the total.

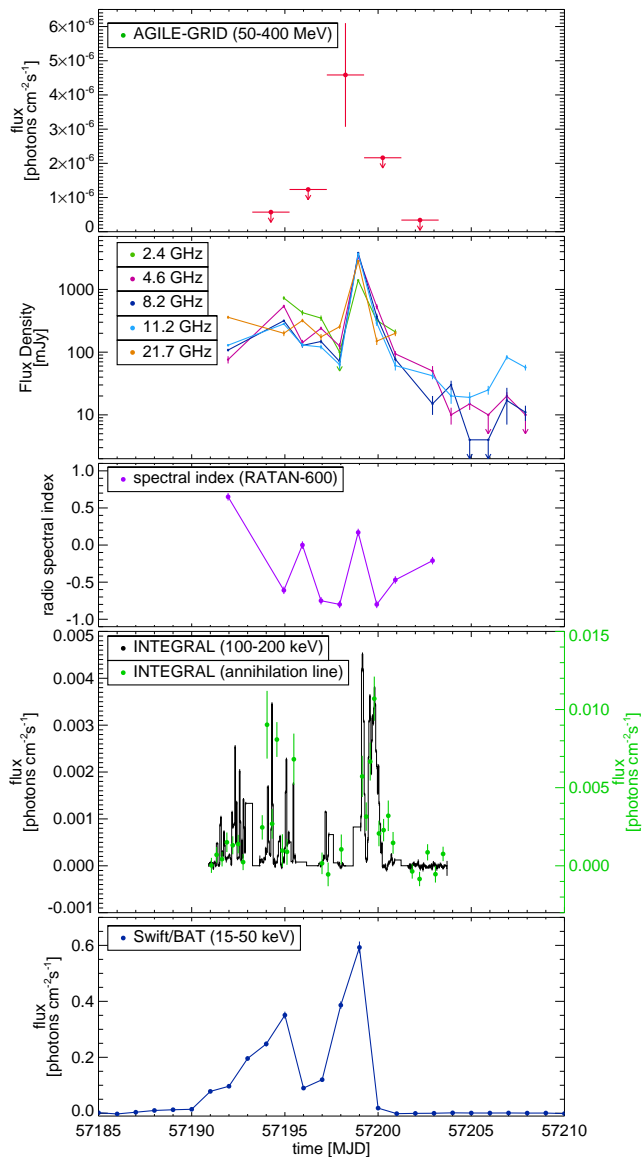


Figure 1. Multiwavelength light-curve throughout the June 2015 outburst of V404 Cyg. From top to bottom: AGILE-GRID 50–400 MeV, 48 hours integration; RATAN-600 radio flux density (2.4, 4.6, 8.2, 11.2 and 21.7 GHz); RATAN-600 radio spectral index (4–11 GHz); INTEGRAL/SPI continuum (100–200 keV, black histogram) and annihilation line (green points), data from Siegert et al. (2016); Swift/BAT 15–50 keV, 1-day bin.

consistent with a microquasar behavior, in which transient jets are responsible for the high-energy γ -ray emission (see Section 3.2). While the hard X-ray emission monitored by *Swift*/BAT in the 15–50 keV range is fully dominated by the disk-corona activity, the radio (RATAN-600) and soft/HE γ -ray radiation (INTEGRAL/SPI and AGILE-GRID) clearly indicate the

presence of a relativistic jet. INTEGRAL/SPI detected three time intervals of enhanced continuum emission at 100–200 keV (MJD: ~ 57190.9 – 57192.9 , ~ 57193.6 – 57195.6 , and ~ 57199.1 – 57200.9). In particular, the second and third intervals show an evident correlation with the 511 keV pair-annihilation emission, suggesting the presence of an unstable antiparticle outflow possibly related to the jet production (Siegert et al. 2016). Radio flux density evolution, as detected by RATAN-600, shows a first peak (~ 0.5 Jy at 4.6 GHz) coincident with the second burst activity observed by INTEGRAL/SPI (~ 57195.0). A giant radio flare (~ 3.4 Jy at 4.6 GHz) is detected during the last and brightest peak emission measured by INTEGRAL/SPI (~ 57199.2), which is consistent with the γ -ray flare detected by the AGILE-GRID.

The AGILE observations are compatible with the *Fermi*-LAT measurements, reported in Loh et al. 2016 and in Appendix A. The contemporaneous burst observation of V404 Cyg by AGILE and *Fermi* gives statistical robustness to this episode, even though the detection significance is not impressive if considered individually. Moreover, the identification of V404 Cyg is secured by the time correlation with a strong outburst detected from the system at other wavelengths.

The multiwavelength behavior suggests that HE γ -ray activity is associated only with the highest activity phase of plasma ejection in the jet. In a jet scenario, the observed HE γ -rays must be produced outside the hot and dense corona region that is opaque (due to $e^+ e^-$ pair production) for photon energies $E \gg m_e c^2$. According to this picture, HE γ -rays produced in the innermost part of the jet are converted to pair plasma. There is a continuous creation and annihilation of plasma close to the central source, forming a broad annihilation line (Siegert et al. 2016; Loh et al. 2016). Outside the coronal plasma, when the plasmoid moves away from the central source along the jet, HE γ -rays can propagate outwards without strong absorption (see, for a quantitative analysis applied to the specific case of Cyg X-3, Cerutti et al. 2011).

In Fig. 4 the Spectral Energy distribution (SED) at the outburst time is presented, showing INTEGRAL, AGILE and *Fermi*-LAT data.

3.2. Microquasar scenario

As discussed above, the multifrequency emission pattern throughout the outburst clearly resembles the one observed for Cyg X-3 (γ -ray flares detected during X-ray spectral transitions and preceding giant radio outbursts, Corbel et al. 2012; Piano et al. 2012). The peak γ -ray isotropic luminosity for Cyg

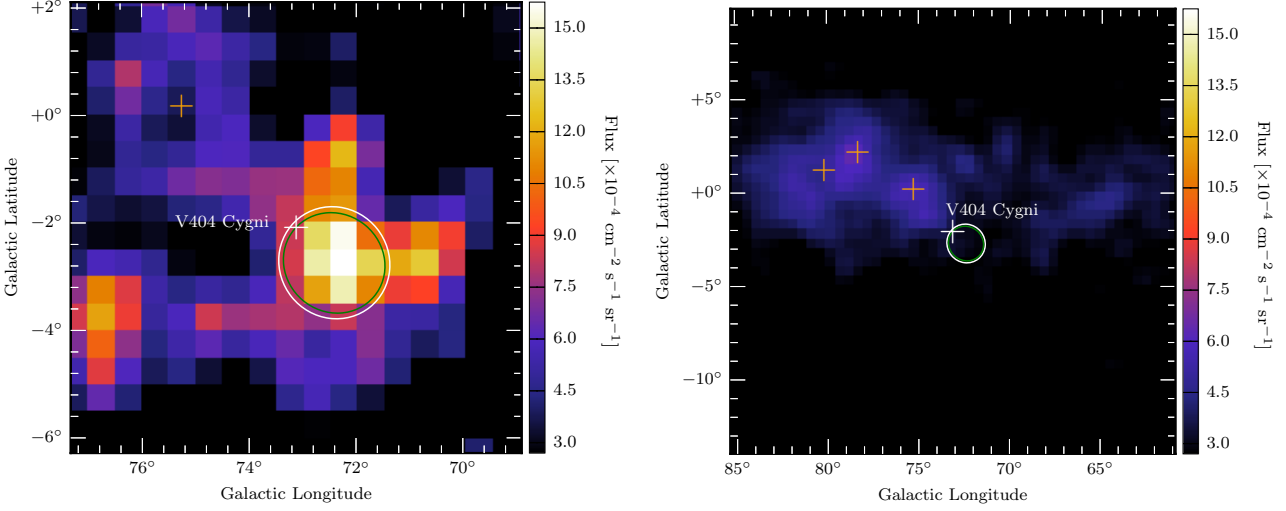


Figure 2. *Left panel:* AGILE-GRID γ -ray intensity map in Galactic coordinates with a three-pixel Gaussian smoothing. Photon energy: 50–400 MeV. Integration time: 2015-06-20 UT 06:00:00 – 2015-06-30 UT 06:00:00. Pixel size: 0.5° . Green contour: 95% confidence region. White contour: statistical + systematic (0.1°) containment region. White cross: optical position of V404 Cyg. *Right panel:* The quiescent phase of V404 Cyg – with the same characteristics of the left panel, but different size – from 2015-01-01 UT 12:00:00 to 2015-06-01 UT 12:00:00. The three pulsars included in the multi-source analysis are marked with magenta crosses (from left to right: PSR J2032+4127, PSR J2021+4026, and PSR J2021+3651). The white cross is the optical position of V404 Cyg. The white contour is the AGILE containment region of the flaring source (stat + syst). The color bar is the same for both the maps.

X-3 was found to be $L_\gamma \sim 10^{36} \text{ erg s}^{-1}$ (for $E_\gamma \geq 100$ MeV and a distance of 7–10 kpc, [Tavani et al. 2009b](#); [Fermi LAT Collaboration et al. 2009](#)). It was found

that both a leptonic (inverse Compton, IC) and hadronic (π^0 -decay) scenario can account for the HE γ -ray emission, although IC processes can explain in a more natural way the γ -ray modulation and the multi-wavelength links ([Dubus et al. 2010](#); [Piano et al. 2012](#); [Sahakyan et al. 2014](#)).

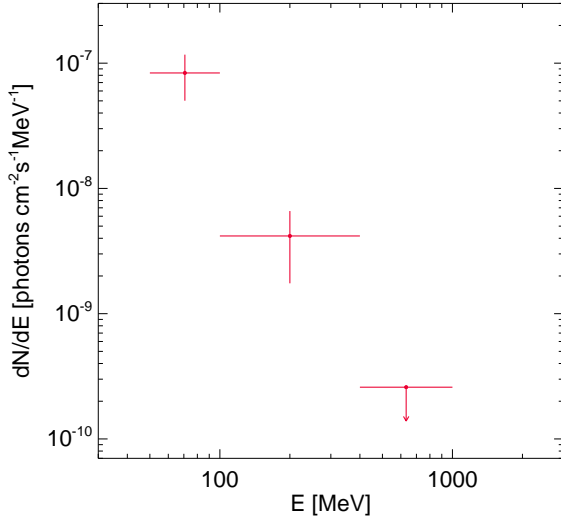


Figure 3. Differential γ -ray spectrum from V404 Cyg as detected by the AGILE-GRID during the peak emission activity, 2015-06-24 UT 06:00:00 to 2015-06-26 UT 06:00:00 (MJD 57197.25–57199.25). The flux UL is a 68% C. L. value.

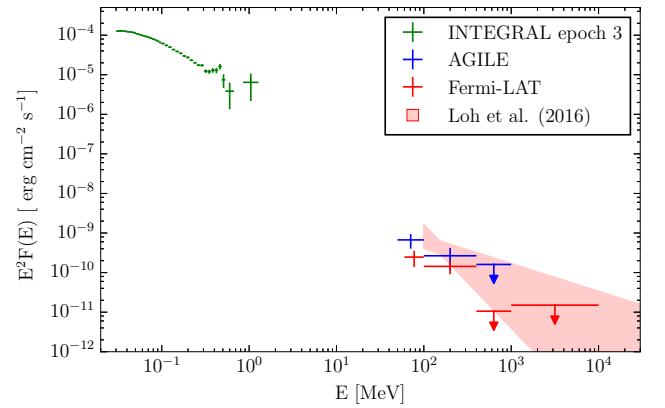


Figure 4. Multifrequency SED of V404 Cyg during the outburst phase. *Green points:* INTEGRAL data, MJD ~ 57199.1 – 57200.9 (epoch 3 in [Siebert et al. 2016](#)); *Blue points:* AGILE data, MJD 57197.25–57199.25, *Red points:* Fermi-LAT data (see Appendix A), MJD 57198.75–59199.75. *Red shaded region:* 6h peak spectrum from [Loh et al. \(2016\)](#), \sim MJD 57199.1 – 57199.3. The flux ULs are 68% C.L. values.

In V404 Cyg, the simultaneous detection of HE γ -rays, $e^+ e^-$ annihilation emission and a strong radio outburst can support a microquasar scenario with a dominant leptonic component responsible for the observed pattern of emission (at radio, hard-X/soft- γ -ray and HE γ -ray frequencies).

In this work, for V404 Cyg we found a peak γ -ray luminosity $L_\gamma \sim 10^{35}$ erg s $^{-1}$, for $50 \leq E_\gamma \leq 400$ MeV and for a source distance of 2.39 kpc. According to the γ -ray observations by AGILE and *Fermi*-LAT, $L_\gamma \sim 10^{-4} L_{Edd}$ in V404 Cyg, which turns out to be a weaker γ -ray emitter with respect to Cyg X-3. Nevertheless, we have indications of a soft-spectrum HE γ -ray emission with no significant signal observed above 400 MeV. If we take into account the strong emission detected up to soft γ -rays by INTEGRAL and compare it with the low significance HE γ -ray flux detected by the AGILE-GRID and *Fermi*-LAT, we could ask ourselves whether the bulk γ -ray radiation is concentrated in the energy band between 1 and 50 MeV, a frequency window that current γ -ray detectors cannot observe. By a qualitative extrapolation to this energy range – based on the observed trend (see Fig. 4) – we could expect an energy flux around $\sim 10^{-8} - 10^{-6}$ erg cm $^{-2}$ s $^{-1}$. Is there a strong energy cut-off in the HE emission (indicating an upper limit to the Lorentz factor of the emitting particles in the jet)? Is the same spectral component responsible for the hard X-ray and γ -ray radiation? The next generation of γ -ray detectors, such as the e-ASTROGAM space mission (Tatischeff et al. 2016), will be able to explore this energy range with a good sensitivity, trying to disentangle the HE emission scenario for this kind of astrophysical sources.

APPENDIX

A. FERMI-LAT DATA ANALYSIS

In this appendix we analyzed the *Fermi*-LAT (Atwood et al. 2009) data using the *Fermi* Science Tools v10r0p5⁴ and the user contributed package *enrico*⁵. We analyzed the data between 2015 June 17 UT 18:00:00 (MJD 57190.75) and 2015 July 02 UT 18:00:00 (MJD 57205.75), covering the peak activity period reported at other wavelengths.

We selected data with the P8R2_TRANSIENT_v16 class in the widest energy range, given the expected faint short-lived activity of this binary in the gamma-ray domain. The data were centered at the position of V404 Cyg and extended within a region of interest (ROI) of 25° radius. We adopted the last Galactic diffuse emission model (gll_iem_v06.fits) and the isotropic model (iso_P8R2_SOURCE_V6_v06.txt) in a likelihood analysis, and the 3rd point source catalog gll_psc_v16.fit (Acero et al. 2016). In the model, the Galactic diffuse and isotropic components are fixed to the values that we obtained in a long-time integration (1 month) preceding the active phase of June 2015. We selected PASS8 FRONT and BACK transient event class. We limited the reconstructed ZENITH_ANGLE to be less than 90° (equivalent to an Earth albedo filtering angle of 75°) to strongly reduce γ -rays coming from the Earth's atmosphere. The good time intervals were selected so that the instrument rocking angle was lower than 52°.

⁴ <http://fermi.gsfc.nasa.gov>

⁵ <https://github.com/gammapy/enrico/>

4. ACKNOWLEDGEMENTS

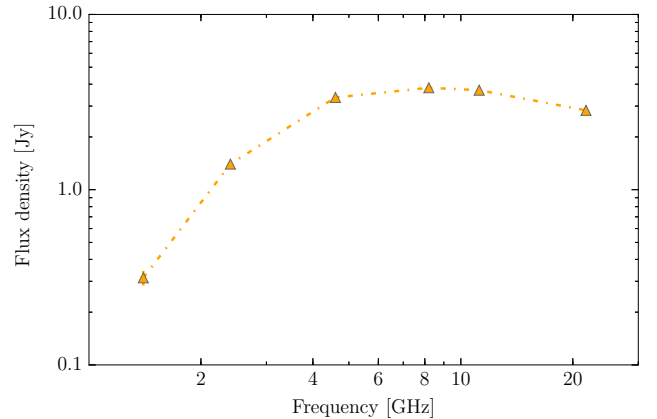


Figure 5. Radio spectrum of the outburst phase (MJD 57198.93) as observed by RATAN-600 (Trushkin et al. 2015).

AGILE is an ASI space mission developed with programmatic support by INAF and INFN. This study was carried out with partial support through the ASI grant no. I/028/12/2.

The authors thank the anonymous referee for her/his stimulating comments on the manuscript and T. Siegert for providing the INTEGRAL data showed in Fig. 1 and 4 (previously published in Siegert et al. 2016).

Software: MSLA (Bulgarelli et al. 2012), Fermi Science Tools v10r0p52 (<http://fermi.gsfc.nasa.gov>), *enrico* (<https://github.com/gammapy/enrico/>)

In the data modeling, we took into account nearby sources up to distances of 25° . The analysis procedure was divided into two steps: in the first one, all sources closer than 6° to V404 Cyg had all of their spectral parameters free, while sources further away had their parameters fixed. A likelihood analysis using the Minuit optimizer was run, determining the best fit parameters for our source and the nearby sources. In a second step, we fixed the spectral parameters for all the sources, except for V404 Cyg, to the ones found in the first step, and run the likelihood analysis again in order to obtain a refined fit. For V404 Cyg we used a simple power law model.

We produced light-curves with 24h time bins in two different energy bands: 60–400 MeV, and above 400 MeV. No significant emission was detected above 400 MeV. In the 60–400 MeV light-curve, instead, we obtained a hint of a detection at $TS=13.4$ ($\sim 3.7\sigma$, see Fig. 6) and a γ -ray flux $F_\gamma = (1.4 \pm 0.4) \times 10^{-6}$ photons $\text{cm}^{-2} \text{s}^{-1}$ for the time integration between 2015-06-25 UT 18:00:00 and 2015-06-26 UT 18:00:00 (MJD 57198.75–59199.75). This result is fully consistent (in flux and integration time) with the 12h peak emission found by Loh et al. (2016) in their analysis of the *Fermi*-LAT data in the 100 MeV – 100 GeV energy range.

A.1. *AGILE*–*Fermi* comparison

By comparing the *AGILE-GRID* and our independent *Fermi*-LAT analysis, we can note that both γ -ray instruments found a quasi-simultaneous peak emission with a time overlap of 12h. The *AGILE-GRID* and *Fermi*-LAT γ -ray fluxes observed at the peak emission are consistent with each other at 2σ C.L..

AGILE and *Fermi* have different sky-scanning strategies and, consequently, they observe the target source at different times and for different duration in every single scan. Thus, if the γ -ray emission time is short (sub-hour variability as in the optical and X-ray frequencies), the detectors can miss part of the peak activity if the source is outside the field of view during the γ -ray activity.

Fig. 7 shows the *AGILE-GRID* and *Fermi*-LAT time evolution of the V404 Cyg off-axis angle during the period 2015-06-24 UT 06:00:00 and 2015-06-26 UT 18:00:00 (MJD 57197.25–59199.75), union of the γ -ray peak emission time intervals found by two instruments. As noticed in other studies, *AGILE* and *Fermi* can have different exposure on specific target (Sabatini et al. 2013; Munar-Adrover et al. 2016).

REFERENCES

- | | |
|-------------------------------------------------------------------------------------------------------------------------------------------------------------------------------------------------------------------------------------------------------------------------------------------------------------------------------------------------------------------------------------------------------------------------------------------------------------------------------------------------------------------------------------------------------------------------------------------------------------------------------------------------------------------------------------------------------------------------------------------------------------------------------------------------------------------------------------------------------------------------------------------------------------------------------------------------------------------------------------------------------------------------|--------------------------------------------------------------------------------------------------------------------------------------------------------------------------------------------------------------------------------------------------------------------------------------------------------------------------------------------------------------------------------------------------------------------------------------------------------------------------------------------------------------------------------------------------------------------------------------------------------------------------------------------------------------------------------------------------------------------------------------------------------------------------------------------------------------------------------------------------------------------------------------------------------------------------------------------------------------------------------------------------------------------|
| <p>Acerro, F., Ackermann, M., Ajello, M., et al. 2016, <i>ApJS</i>, 223, 26</p> <p>Atwood, W. B., Abdo, A. A., Ackermann, M., et al. 2009, <i>ApJ</i>, 697, 1071</p> <p>Barbiellini, G., Fedel, G., Liello, F., et al. 2002, <i>Nuclear Instruments and Methods in Physics Research A</i>, 490, 146</p> <p>Barthelmy, S. D., D’Ai, A., D’Avanzo, P., et al. 2015, <i>GRB Coordinates Network</i>, 17929, 1</p> <p>Bulgarelli, A., Chen, A. W., Tavani, M., et al. 2012, <i>A&A</i>, 540, A79</p> <p>Casares, J., Charles, P. A., & Naylor, T. 1992, <i>Nature</i>, 355, 614</p> <p>Casares, J., & Charles, P. A. 1994, <i>MNRAS</i>, 271, L5</p> <p>Cerutti, B., Dubus, G., Malzac, J., et al. 2011, <i>A&A</i>, 529, A120</p> <p>Corbel, S., Dubus, G., Tomsick, J. A., et al. 2012, <i>MNRAS</i>, 421, 2947</p> <p>Dubus, G., Cerutti, B., & Henri, G. 2010, <i>MNRAS</i>, 404, L55</p> <p><i>Fermi</i> LAT Collaboration, Abdo, A. A., Ackermann, M., et al. 2009, <i>Science</i>, 326, 1512</p> | <p>Hynes, R. I., Bradley, C. K., Rupen, M., et al. 2009, <i>MNRAS</i>, 399, 2239</p> <p>Jenke, P. A., Wilson-Hodge, C. A., Homan, J., et al. 2016, <i>ApJ</i>, 826, 37</p> <p>Khargharia, J., Froning, C. S., & Robinson, E. L. 2010, <i>ApJ</i>, 716, 110</p> <p>Kimura, M., Isogai, K., Kato, T., et al. 2016, <i>Nature</i>, 529, 54</p> <p>Loh, A., Corbel, S., Dubus, G., et al. 2016, <i>MNRAS</i>, 462, L111</p> <p>Makino, F., Wagner, R. M., Starrfield, S., et al. 1989, <i>IAUC</i>, 4786, 1</p> <p>Mattox, J. R., Bertsch, D. L., Chiang, J., et al. 1996, <i>ApJ</i>, 461, 396</p> <p>Miller-Jones, J. C. A., Gallo, E., Rupen, M. P., et al. 2008, <i>MNRAS</i>, 388, 175</p> <p>Miller-Jones, J. C. A., Jonker, P. G., Dhawan, V., et al. 2009, <i>ApJL</i>, 706, L230</p> <p>Munar-Adrover, P., Sabatini, S., Piano, G., et al. 2016, accepted for publication in <i>ApJ</i>, arXiv:1607.03006</p> <p>Muñoz-Darias, T., Casares, J., Mata Sánchez, D., et al. 2016, <i>Nature</i>, 534, 75</p> |
|-------------------------------------------------------------------------------------------------------------------------------------------------------------------------------------------------------------------------------------------------------------------------------------------------------------------------------------------------------------------------------------------------------------------------------------------------------------------------------------------------------------------------------------------------------------------------------------------------------------------------------------------------------------------------------------------------------------------------------------------------------------------------------------------------------------------------------------------------------------------------------------------------------------------------------------------------------------------------------------------------------------------------|--------------------------------------------------------------------------------------------------------------------------------------------------------------------------------------------------------------------------------------------------------------------------------------------------------------------------------------------------------------------------------------------------------------------------------------------------------------------------------------------------------------------------------------------------------------------------------------------------------------------------------------------------------------------------------------------------------------------------------------------------------------------------------------------------------------------------------------------------------------------------------------------------------------------------------------------------------------------------------------------------------------------|

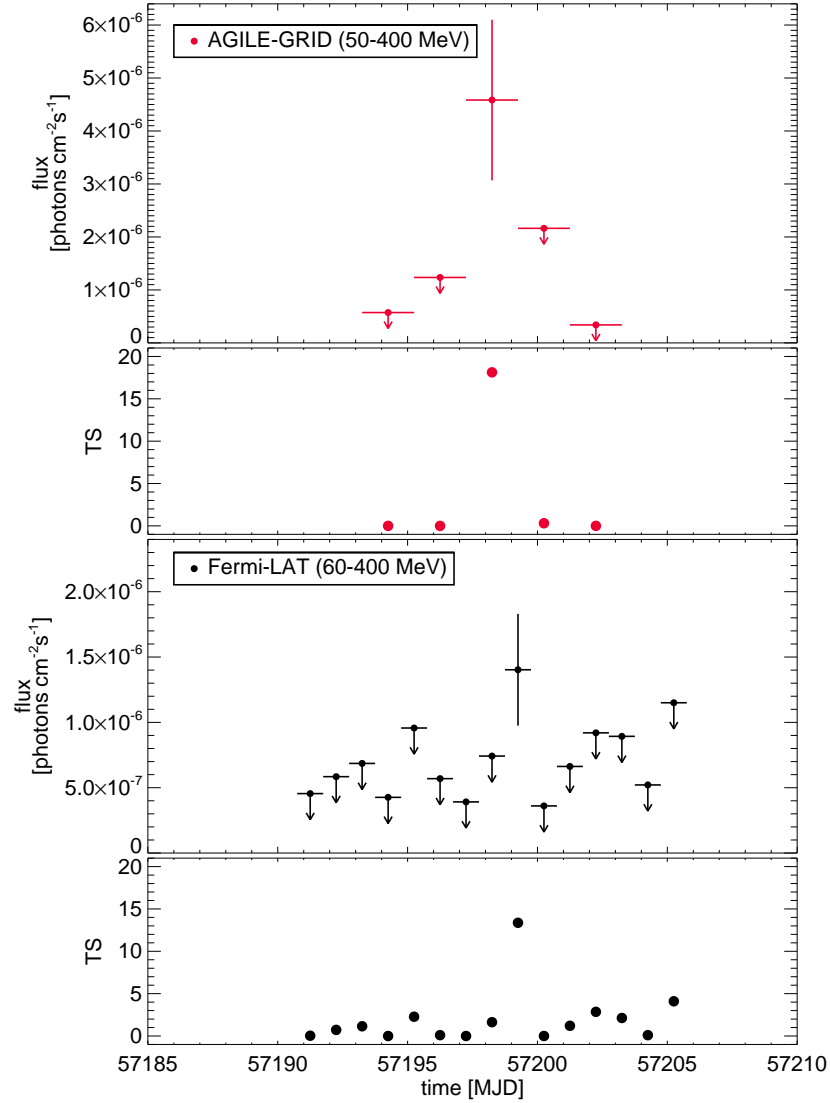


Figure 6. HE γ -ray light-curves across the V404 Cyg peak emission. From top to bottom: AGILE-GRID 48h-bin light-curve (50–400 MeV energy band); AGILE-GRID TS of each time-bin; Fermi-LAT 24h-bin light-curve (60–400 MeV energy band); Fermi-LAT TS for each time-bin. For both AGILE and Fermi, flux error bars and flux ULs are 68% C. L. values.

Piano, G., Tavani, M., Vittorini, V., et al. 2012, A&A, 545, A110
 Pittori, C., Verrecchia, F., Chen, A. W., et al. 2009, A&A, 506, 1563
 Prest, M., Barbiellini, G., Bordignon, G., et al. 2003, Nuclear Instruments and Methods in Physics Research A, 501, 280
 Rana, V., Loh, A., Corbel, S., et al. 2016, ApJ, 821, 103

Rodriguez, J., Cadolle Bel, M., Alfonso-Garzón, J., et al. 2015, A&A, 581, L9
 Sabatini, S., Tavani, M., Coppi, P., et al. 2013, ApJ, 766, 83
 Sabatini, S., Donnarumma, I., Tavani, M., et al. 2015, ApJ, 809, 60
 Sahakyan, N., Piano, G., & Tavani, M. 2014, ApJ, 780, 29
 Segreto, A., Del Santo, M., D’Aí, A., et al. 2015, The Astronomer’s Telegram, 7755

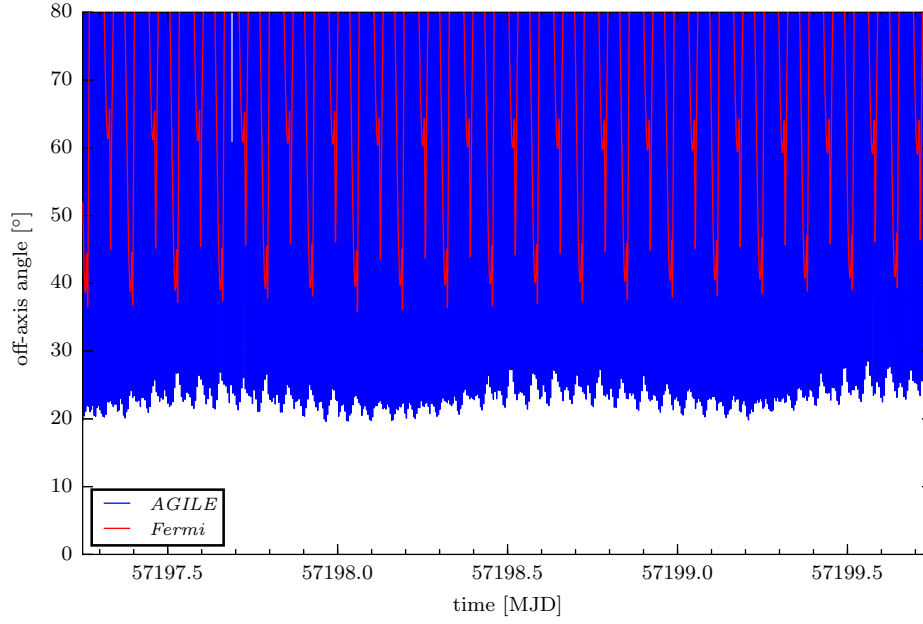


Figure 7. AGILE-GRID (blue) and *Fermi*-LAT (red) time evolution of the V404 Cyg off-axis angle, for the period 2015-06-24 UT 06:00:00 and 2015-06-26 UT 18:00:00 (MJD 57197.25–59199.75), union of the γ -ray peak emission time intervals found by AGILE and *Fermi* (see Fig.5 6).

Shahbaz, T., Ringwald, F. A., Bunn, J. C., et al. 1994,

MNRAS, 271, L10

Siegert, T., Diehl, R., Greiner, J., et al. 2016, Nature, 531,

341

Tatischeff, V., Tavani, M., von Ballmoos, P., et al. 2016,
Proc. SPIE 9905, Space Telescopes and Instrumentation
2016: Ultraviolet to Gamma Ray, 99052N

Tavani, M., Barbiellini, G., Argan, A., et al. 2009, A&A,
502, 995

Tavani, M., Bulgarelli, A., Piano, G., et al. 2009, Nature,
462, 620

Trushkin, S. A., Nizhelskij, N. A., & Tsybulev, P. G. 2015,
The Astronomer’s Telegram, 7716